Ripples formed in the sputter erosion of Pd(111)



2003 J. Phys.: Condens. Matter 15 L735

(http://iopscience.iop.org/0953-8984/15/49/L01)

INSTITUTE OF PHYSICS PUBLISHING JOURNAL OF PHYSICS: CONDENSED MATTER

J. Phys.: Condens. Matter **15** (2003) L735–L742 PII: S0953-8984(03)66603-8

**LETTER TO THE EDITOR**

# Ripples formed in the sputter erosion of Pd(111)

**M Ondrejcek, W Swiech, M Rajappan and C P Flynn**

Physics Department and Materials Research Laboratory, University of Illinois at Urbana-Champaign, 1110 West Green Street, Urbana, IL 61801, USA

Received 29 July 2003
Published 25 November 2003
Online at stacks.iop.org/JPhysCM/15/L735

**Abstract**

During the sputter erosion of Pd(111) by 1 keV $Ar^+$ ions in the temperature range ∼800–1000 K we observe the development of clearly defined ridges that deepen as sputtering continues up to ∼200 ML removed. Step edges observed by low energy electron microscopy appear as contour lines that define the detailed topography of the rippled surfaces. Different characteristic step profiles, and hence surface geometries, are observed after short and long sputtering times. The sequence resembles the interfacial structures reported for the Mullins–Sekerka instability of driven solidification interfaces. At long sputtering times the ridges adopt crystallographic orientations, as reported in recent studies of the ion erosion of crystal surfaces.

## 1. Introduction

Several recent papers review a symmetry breaking in which sputtering causes an initially flat surface to evolve into a rippled surface structure [1–5]. The background to the field in surface science is described in monographs [6, 7]. It has been noted that the phenomena are similar to interfacial processes in which an initially flat interface adopts quasi-periodic or cellular structure. Similar instabilities appear during epitaxial growth in the step flow regime [7]. Model treatments separately identify the Mullins–Sekerka instability [8] of interfacial growth fronts, and the Bales–Zangwill instability [9], during growth, of surface step edge profiles, with rather similar causes. The direction of the driven growth is the factor that breaks the symmetry. In the present case of surface ripples formed during erosion by sputtering, the detailed description of the process remains yet to be established. For crystals (rather than amorphous materials [1, 10]) the orientation of the ripples is often crystallographic, along close packed rows [5], rather than being determined by the orientation of the ion beam relative to the surface. The ripple periodicity scales weakly with sputtering exposure. Elaborate descriptions have been attempted [11]. However, it is not clearly established whether the ripples arise from kinetics or from dynamical effects. An example of the former might be from defect flow, with direction dependence introduced by the Ehrlich–Schwoebel barrier [7] at steps. Dynamical processes, such as focused collision sequences in the ion–crystal interactions, can, alternatively, introduce crystallographic dependences into damage events [12–15].

  

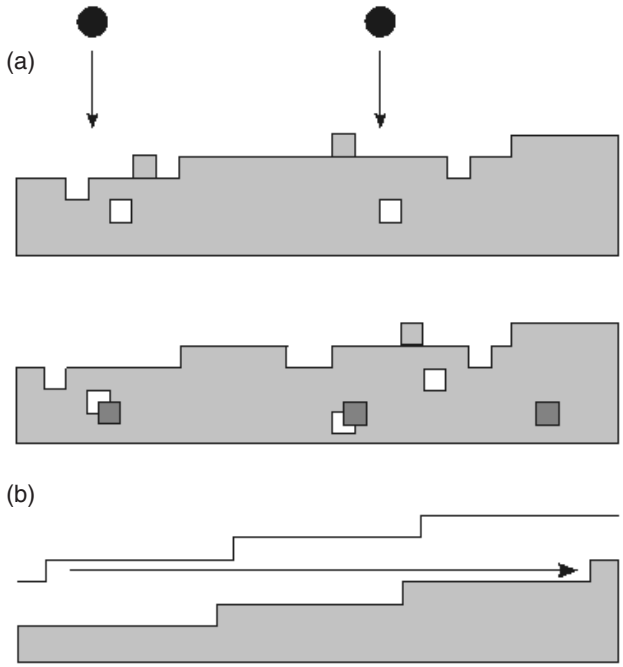


**Figure 1.** In (a), the typical damage created by a low energy ion impact is sketched, with bulk vacancies and interstitials formed, and surface adatoms and advacancies, in addition to ions sputtered into the vacuum. The same surface is shown again after adatom annealing. (b) shows the mean field model of erosion, with enough surface diffusion that the surface after erosion is equivalent to the surface before erosion (upper line), with merely step flow through a distance that corresponds to the monolayers removed (here 3 ML).

In this letter we describe ripples detected by low energy electron microscopy (LEEM) on Pd(111) irradiated using 1 keV $Ar^+$ ions. In a field typically microns in extent, LEEM makes surface steps clearly visible at 10 nm resolution (for a collection of recent articles on LEEM and applications see [16]). It thereby offers a sensitive view of ripple formation in its early stages. Using progressive cycles of sputtering at different temperatures, and subsequent annealing to restore a flat surface, we have been able to follow the initial phases of ripple formation for a range of sputtering doses and temperatures. Several new features of the rippling mechanism and its relationship to similar symmetry breaking in other contexts (see [8, 9]), mentioned above, have thereby been recognized. This letter provides a brief summary of the observations and their interpretation.

It is possible to conduct an erosion process such that the effects of the ion beam are under fairly close control. Typically, the ion beams employed in erosion, of energy $\sim$1 keV, induce surface displacement processes and create surface and bulk point defects but not deep damage. Simulation of $Ar^+$ 1 keV impact on Pt(111) is thought to sputter off four atoms from one ion impact [17], to also create seven bulk vacancies and a small fraction of one interstitial confined to the top few layers, and to leave perhaps ten new adatoms and nine new surface advacancies. The asymmetry between surface antidefects (i.e., advacancies and adatoms) arises because the weakly bound adatoms are most easily sputtered off into the vacuum. Figure 1(a) is a sketch showing the result of a typical ion impact on a flat terrace. Recombination of bulk and surface antidefects takes place progressively more rapidly as the sample sputtering temperature, $T$, is

raised. This occurs first for the more mobile surface defects and then, at longer times or still higher temperatures, for the bulk defects, specifically vacancies and interstitials.

In our research we identify a temperature at which the surface mobility is sufficient that surface recombination does take place locally, while bulk and long range surface processes remain frozen or sluggish. Our criterion is that local recombination is sufficiently rapid that step edges remain well defined and clearly visible by LEEM throughout the sputtering process.

In the regime thus identified, experiments on the erosion of a smoothly stepped surface become clearly defined. Given local recombination, the average effect of 3 ML of erosion, for example, is to reproduce the initial surface, simply three layers lower. This is sketched in figure 1(b). It is true that the ion beam also introduces damage that remains behind partly unannealed. A point of importance here is that the damage is confined to the outer layers and is entirely sputtered away with those layers. Therefore the 'mean field' model surface described by this process rapidly comes to a steady state of constant surface and bulk damage, and is otherwise characterized merely by step edges advancing, in the uphill direction, by one step spacing each sputtered monolayer.

The phenomena of interest in this letter constitute departures from the mean field model caused by instabilities through which the actual surface develops ripples. These departures from the mean field thus resemble cellular structures found in driven, initially planar, solid–liquid interfaces or of straight steps during epitaxial growth. In order to conform with this model framework, the experiments described below were undertaken on clean, regularly stepped surfaces, and with sputter exposures varying in the range from ten to several hundreds of monolayers, in which the ripples first nucleate and grow.

## 2. Experiments

A Pd crystal 9 mm in diameter and 1 mm thick, oriented (111), and miscut by about 0.07°, was purchased from Surface Preparation Laboratory, The Netherlands. The surface step normal lay on average approximately 13° from the close packed direction and the steps were separated by ∼170 nm. Repeated sputter–anneal cycles using 1 keV $Ar^+$ ions with oxygen were employed to relax and clean the surface, until the steps became regularly spaced and contaminants fell below the detection level for Auger analysis (<1%). Depth profiling experiments following extensive sputtering with the Pd surface masked, apart from a narrow slit, were employed to calibrate the sputtering depth in terms of sputtering exposure (i.e., beam current and time). In what follows, the exposures are quoted in monolayers (MLs) sputtered.

The erosion reported here employed an ion beam at 35° to the surface plane, with two azimuths studied differing by 90°. With an Ar pressure of $5 \times 10^{-8}$ Torr, typical ion currents of 0.5 $\mu$A cm$^{-2}$ gave erosion rates of about 9 ML min$^{-1}$. We employed total erosion in the range 18–180 ML at temperatures below ∼1000 K. After erosion, samples were cooled to room temperature and positioned for LEEM viewing. Prior to each new bombardment the crystal was heated to 1300 K to recover the smooth surface, and a full cleaning cycle with oxygen was performed every 15 cycles.

Surfaces were examined in a LEEM instrument designed by Tromp [18] and described elsewhere [19]. Electron beam impact on the sample rear was used for heating; in the present research the temperatures were limited to 1300 K by the thermal conductivity of the Pd crystal. A typical LEEM image of the relaxed Pd surface, with 2.6 $\mu$m field of view, is presented as figure 2. The regularly spaced lines are single step edges observed with ∼10 nm lateral resolution. The steps run uphill from right to left, almost normal to the close packed $[\bar{1}2\bar{1}]$ direction.

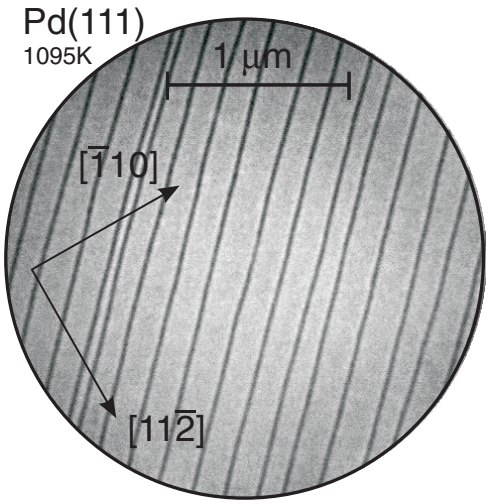


**Figure 2.** LEEM image of the clean, relaxed Pd(111) surface studied in this work. The electron impact energy is 5 eV.

## 3. Results and discussion

Sputtering of Pd(111) with 1 keV $Ar^+$ ions gave results dependent on the ambient temperature. Below 500 K, the damage induced by the ion beam eliminated the visible step structure. Observations were therefore confined to higher temperatures, where local recovery by surface diffusion preserved a visible step structure. Then sputtering, in effect, caused defined steps to flow in the uphill direction by as many step spacings as the atomic layers removed by the ion beam. Above about 1000 K, surface diffusion proved sufficiently rapid to damp most sputtering modifications of the step profile. In between 600 and 900 K, the character of the rippling changed between small doses and large doses, with the boundary at $S \sim 30$ ML. Important crystallographic effects were also clearly recorded. Experience with annealing at temperatures at and above the sputtering temperatures indicates that step profiles remained essentially frozen between sputtering and initial viewing.

Figure 3(a) illustrates the type of step profile observed for small net sputtering. Steps are seen to adopt substantially sinusoidal profiles with amplitudes comparable with the step spacing. A view at increased magnification, with the same net erosion, is given in figure 3(b). Successive steps generally have similar perturbed wavelengths and amplitudes. This could reasonably be a consequence of each step separately responding to a common inherent instability in a similar way during step flow. However, the fact that the waves on successive steps are in phase, with peaks aligned, provides a strong indication that, in addition, an interaction occurs between neighbouring steps. The point is that the crystal possesses translational invariance along the steps and, in the absence of an organizing interaction, the phases on successive steps would differ randomly.

Among the possible origins of correlated perturbations on successive steps one must include the possibility of both direct and indirect effects. For example, during erosion-induced step flow, successive steps pass over the same area of surface, so that correlated profiles could possibly be created indirectly by surface inhomogeneities such as small defect assemblies or impurity distributions that are not visible in the LEEM images. In the present case this type of explanation is consistent with the observations because the correlations extend typically over distances smaller than the step flow induced by the sputtering. Thus, in the case of figures 3(a)

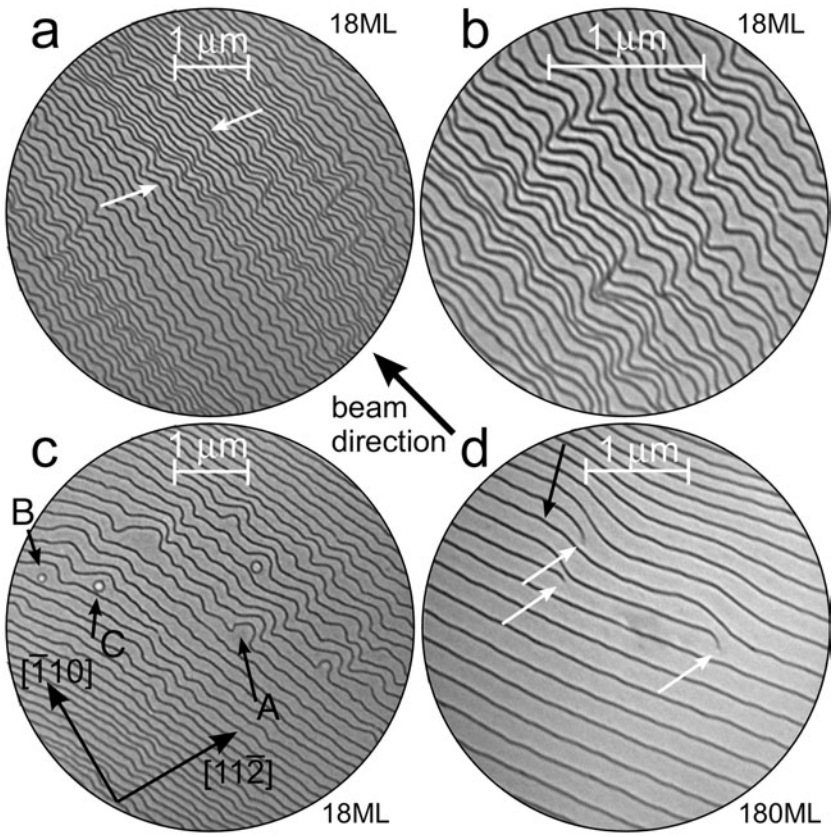


**Figure 3.** LEEM images of a Pd(111) surface after sputtering. (a) After 18 ML erosion at 800 K, successive steps show correlated features (as marked, for example, by the arrows) over distances of ∼10 steps. (b) An image at higher resolution. (c) Similar to (a), with islands (e.g. A) and other anomalies (e.g. B, C) starting long sequences of perturbed steps along the direction of flow. (d) Steps perturbed by flow past screw dislocations (white arrows) at 1010 K, with rapid step smoothing from fast diffusion. The added step edge is marked by black arrow.

and (b), the correlations clearly extend over ∼10–20 steps whereas the step displacement from the known sputter depth of 18 ML is, of course, ∼18 step spacings or about 3.1 $\mu$m.

An alternative 'direct' explanation could be that physical interactions between neighbouring steps guide the formation of the phased arrays. As energetic interactions generally decrease with separation, however, we observe that larger in-phase fluctuations often occur on those sequences of steps that have greater separations, and this makes the explanation appear less probable. Terrace diffusion fields of irradiation-induced defects, as they anneal to step edges, provide one illustrative mechanism for physical interactions that could link successive step profiles [20].

That ridges actually nucleate early in erosion from small heterogeneities, and propagate from one step to the next as steps flow, is established directly by observations for these small total fluences. Figure 3(c) provides an example in which sequences of relatively straight steps are interrupted by an island surrounded by a step, for example at the arrow marked A, or else a bulged-out terrace where perhaps an island has just annealed away, for example at B and C. Here the important feature is that a number of subsequent steps along the direction of erosion-induced flow clearly exhibit related in-phase peaks from their past encounters with the same

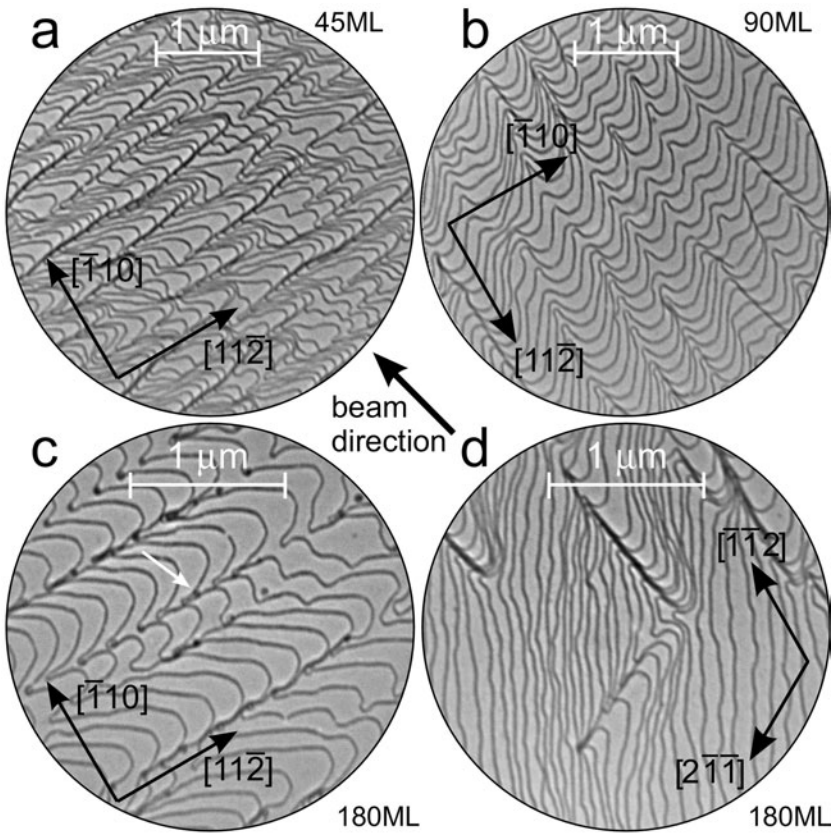


**Figure 4.** (a) After 45 ML erosion at 800 K, the steps develop asymmetrical perturbations. In some cases these become fairly regular, and develop sharp points on the downhill peaks, as seen in (b). (c) reveals precipitates (arrow) that form at the points after 180 ML erosion, much as in driven solidification at interfaces. The crystallographic character of the alignment in the later stages of ripple formation is illustrated in (d) by a case in which two orientations occur, both crystallographic (see the axes provided), and symmetrical to the local step normal. (a) and (c) are rotated by about 90° from (b) and (d).

heterogeneity. The number of perturbed steps is smaller than the sputtered depth of 18 ML. We believe that the nucleating features may themselves be erosion induced since they appear to be absent from the relaxed surface before sputtering (see figure 2).

A compelling example of similar propagation, even at a higher sputtering temperature of 1010 K, is given in figure 3(d). There successive steps have been perturbed as they flowed past stationary screw dislocations, indicated by white arrows. Threading screw dislocations cause a local one-plane displacement normal to the surface and hence each introduces an added step edge marked in the image (black arrow). The temperature is sufficiently high that nonlinear structure is quickly suppressed. In the response to the screw dislocation the flowing steps are disturbed, but diffusion smoothes out the perturbed profiles progressively for steps that passed the screw by flow further in the past. The considerable diffusive smoothing in the duration of a single monolayer of sputtering (i.e. one step spacing) shows clearly how diffusion processes must entirely eliminate short period waves (e.g. figure 3(b)) at these elevated temperatures.

Larger ion beam fluences cause progressively greater step perturbations, of a type illustrated in figure 4(a). Here, the symmetry is broken between the up and down step directions.

Since LEEM images offer only indirect evidence for the sense, up or down a step, we have made atomic force microscopy measurements to determine this important fact directly. At larger fluence the steps have profiles (as in figure 4(a)) that remain rounded on the uphill $[11\bar{2}]$ direction, but become progressively more pointed on the downhill side. The contours indicated by step profiles in figure 4(a) thus correspond to ridges with sharp tops and rounded bottoms, much like wind-induced ripples on sand dunes (see, for example, [1]). The steps flow uphill under erosion, and therefore the pointed ends trail behind the general flow of steps. This is an important point in connection with the Mullins–Sekerka instability [8] of driven solid–liquid interfaces in two dimensions, in which profiles greatly resembling figure 4(a) are observed [7]. In the case of solidification the pointed pockets trailing the flow have been identified unambiguously with drag caused by slow diffusion of heterogeneities, which accumulate in the pockets. A heuristic derivation of the cusped diffusion limited shape is given in [7, p 179]. In selected cases the steps observed in the present research grow in very regular pattern with quite sharp points, as seen in figure 4(b).

It is worth mentioning here that while figure 4(a) is indeed a contour map in which step profiles indicate surface topography, the visual impact is somewhat misleading. Inspection of step profiles shows that the 'ridges' are at most a few steps high, while the separation between ridges is a fraction of 1 $\mu$m. Thus the aspect ratio of the ridges is $\sim 10^{-3}$, and the visual impression of steep slopes near the sharp ridge is largely illusory. It is a great asset of the LEEM technique that surface features can be detected with such extreme sensitivity.

In connection with the role of impurities in the Mullins–Sekerka profiles, we report in figure 4(c) the development of observable heterogeneities near the trailing points on the profiles. Arrows in the image indicate the features under discussion. The close similarity of the profiles with the case of the solid–liquid interface, and the clear evidence for small heterogeneities formed at the 'pockets', encourage a belief that the global behaviour has similar origins in the two cases. If this is so then the profile for high fluence is determined by the slow diffusion of the surface species responsible for the heterogeneities in figure 4(c). In this case it is probable that the more mobile adatoms anneal the surface so that step edges remain well defined, while an excess of advacancies lingers behind, impedes step advance and forms the observed precipitates.

A further fact firmly established in our studies is that the ripples in the later stage of sputter erosion are crystallographic in orientation. This is illustrated in figure 4(d). There the ridges occur along two directions symmetrically placed with respect to the step orientation. The arrows in the figure are drawn along close packed directions of the atoms that form the surface layer, as established in our LEEM studies by low energy electron diffraction. The arrows closely follow the ridge crests, and are far from the step normal, along which the sputter-induced step flow is directed. We therefore affirm that the orientations of the ripple structures during later sputtering are fixed by the crystal lattice at the surface. A similar conclusion has been obtained from earlier studies of other surface planes [1, 5]. It is not yet known whether the mechanism that determines the orientation is diffusion related, as in the Ehrlich–Schwoebel effect in transport over steps, or alternatively, is dynamical in origin, through such ion beam processes as focused collision sequences in which ion energy is transmitted along atomic rows [11–15].

## 4. Summary

Using LEEM we have examined ripples formed by ion sputtering of a clean Pd(111) single crystal. During the removal of the first few monolayers, the surface contours revealed by step edge profiles are sinusoidal, with phases aligned on successive terraces. Coherence

extends over generally smaller lengths than the step flow induced by sputtering. At later times the profiles become asymmetrical, resembling interfacial profiles of the Mullins–Sekerka instability during driven solidification. The topology is then similar to sand ripples, with sharp peaks and rounded valley bottoms. In this phase the ripples are oriented near close packed atomic rows of the surface plane.

This research was supported in part by the DOE under grant DEFG02-02ER46011 and was carried out in the Center for Microanalysis of Materials, University of Illinois at Urbana-Champaign, which is partially supported by the US Department of Energy under Award No. DEFG02-91-ER45439.

## References

[1] Valbusa U, Boragno C and de Mongeot F B 2002 *J. Phys.: Condens. Matter* **14** 8153
[2] Carter G 2001 *J. Phys. D: Appl. Phys.* **34** R1 and references therein
[3] Cahill D G 2003 *J. Vac. Sci. Technol.* A **21** S110
[4] Kalff M, Comsa G and Michely T 2001 *Surf. Sci.* **486** 103
[5] Rusponi S, Boragno C and Valbusa U 1997 *Phys. Rev. Lett.* **78** 2795
[6] Zangwill A 1988 *Physics at Surfaces* (Cambridge: Cambridge University Press)
[7] Pimpinelli A and Villain J 1998 *Physics of Crystal Growth* (Cambridge: Cambridge University Press)
[8] Mullins W W and Sekerka R F 1964 *J. Appl. Phys.* **35** 444
[9] Bales G S and Zangwill A 1990 *Phys. Rev.* B **41** 5500
[10] Bradley R M and Harper J M E 1988 *J. Vac. Sci. Technol.* A **6** 2390
[11] Constantini G, Rusponi S, de Mongeot F B, Boragno C and Valbusa U 2001 *J. Phys.: Condens. Matter* **13** 5875
[12] Averback R S and Diaz de la Rubia T 1997 *Solid State Physics* vol 51, ed H Ehrenreich and F Spaepen (New York: Academic)
[13] Wehner G K 1955 *Phys. Rev.* **102** 690
[14] Nelson R S and Thompson M W 1961 *Proc. R. Soc.* A **259** 458
[15] Silsbee R H 1957 *J. Appl. Phys.* **28** 1246
[16] 2002 *3rd LEEM/PEEM Workshop*; *J. Vac. Sci. Technol.* B **20** 2472–549
[17] Gades H and Urbassek H M 1994 *Phys. Rev.* B **50** 11167
[18] Tromp R M and Reuter M 1991 *Ultramicroscopy* **36** 99
[19] Ondrejcek M, Swiech W, Yang G and Flynn C P 2002 *J. Vac. Sci. Technol.* B **20** 2473
[20] Flynn C P 2002 *Phys. Rev.* B **66** 155405